Available online at www.sciencedirect.com
ScienceDirect
Geochimica et Cosmochimica Acta 70 (2006) 4392–4402
Geochimica
www.elsevier.com/locate/gca

The evolution of surface layers formed during chalcopyrite leaching

Sarah L. Harmer [a], Joan E. Thomas [c,1], Daniel Fornasiero [a], Andrea R. Gerson [b,*,1]

[a] *Ian Wark Research Institute, University of South Australia, Mawson Lakes, SA 5095, Australia*
[b] *Applied Centre for Structural and Synchrotron Studies, University of South Australia, Mawson Lakes, SA 5095, Australia*
[c] *Jefferson Laboratory, Newport News, VA 23606, USA*

Received 18 October 2005; accepted in revised form 20 June 2006

Abstract

Chalcopyrite ($CuFeS_2$) leaching in perchloric acid ($HClO_4$) at an initial pH of one and a temperature of 85 °C has been examined. The rate of leaching of Cu and Fe increased progressively over the duration of the experiment. The Cu leach rate was initially greater (up to 24 h) but thereafter the leach rates for Cu and Fe were approximately equal. After 313 h 81% Cu release was achieved at which time the leach experiment was terminated. Only 25% of the available S was released into solution during the leaching process. Surface speciation over the duration of the leach was examined using X-ray photoelectron spectroscopy (XPS), time of flight secondary ion mass spectrometry (ToF-SIMS) and scanning electron microscopy (SEM). As a result, a three-step reaction pathway is proposed. The first oxidation step involves the release of Cu and Fe into solution and the polymerisation of monosulfide (S^{2-}) to polysulfide S_n^{2-}. The subsequent reduction step does not result in the release of cations to solution but does result in the reformation of surface S^{2-} and other short chain polysulfides, which then on further oxidation restructure to form crystalline elemental sulfur (S^0). This final oxidation step is accompanied by further cation release.

1. Introduction

Chalcopyrite ($CuFeS_2$) is the most common and widespread Cu containing mineral. While it is currently the world's primary source of Cu, chalcopyrite also contributes to acid mine drainage. Understanding the oxidation of chalcopyrite in acidic media is therefore important for both copper extraction and environmental remediation.

Traditional sulfide beneficiation processes have consisted of the separation of chalcopyrite from gangue minerals by flotation followed by smelting. In recent years, leaching has been suggested as a viable alternative for metal extraction from low-grade sulfide ores (Prasad and Pandey, 1988). Several dissolution studies have suggested that chalcopyrite leach rates decrease with time and eventually leaching ceases, implying that dissolution is inhibited by the formation of a passivating surface layer (Linge, 1977; Munoz et al., 1984; O'Malley and Liddell, 1986; Barriga et al., 1987; Prasad and Pandey, 1988; Dutrizac, 1989; Hackl et al., 1995; Maurice and Hawk, 1998). The nature of this passivating layer and the mechanism responsible for its formation are not completely understood.

A recent study, by Harmer et al. (2004), using synchrotron radiation X-ray photoelectron spectroscopy (SRXPS) of a pristine chalcopyrite surface (cleaved under vacuum) revealed three distinct contributions to the S 2p spectrum. In addition to fully coordinated bulk S atoms (S $2p_{3/2}$ binding energy of 161.33 eV) two surface components were revealed. Surface monosulfide (S^{2-}) species were attributed as the source of the S $2p_{3/2}$ contribution at 160.84 eV. A second broad S $2p_{3/2}$ contribution at 161.88 eV was attributed to surface polysulfide species (S_n^{2-}) formed due to the reconstruction of S-terminated cleavage surfaces. Nesbitt and Reinke (1999) and Biegelsen et al. (1990) have previously reported the formation

* Corresponding author. Fax: +618 8302 5545.
E-mail address: Andrea.Gerson@unisa.edu.au (A. R. Gerson).
[1] Formerly of the Ian Wark Research Institute, University of South Australia.

0016-7037/$ - see front matter © 2006 Elsevier Inc. All rights reserved.
doi:10.1016/j.gca.2006.06.1555

of polymeric species on cleaved surfaces of metallic sulfides and arsenides.

Surprisingly few surface analytical studies of oxidised or leached chalcopyrite have been carried out in the absence of either bacteria or electrochemical inducement. Iron hydroxy-oxide enrichment has been identified on fractured chalcopyrite surfaces exposed to air (Buckley and Woods, 1984). Holloway et al. (1982) identified Cu rich sulfides in addition to iron hydroxides on polished chalcopyrite surfaces. Hackl et al. (1995) performed X-ray photoelectron spectroscopy (XPS) and Auger electron spectroscopy (AES) on O_2 pressure leached chalcopyrite identifying a Cu–S_n^{2-} layer approximately one μm thick. It was this layer, with a stoichiometry close to CuS_2, that was proposed to be leach-rate determining. An earlier study by Linge (1976) also came to a similar conclusion. Klauber et al. (2001) and Parker et al. (2003) dismissed the possibility of S_n^{2-} formation claiming that only the sulfur species S^{2-}, S_2^{2-} (disulfide), S^0 (elemental sulfur) and SO_4^{2-} (sulfate) are detectable on leached $CuFeS_2$ surfaces. It has been proposed that the formation of an S^0 layer may also act as a diffusion barrier to the transport of ions and electrons (Dutrizac, 1989).

Atmospheric and electrochemical studies of chalcopyrite by Yin et al. (1995, 2000) are in agreement with Buckley and Woods (1984). Yin et al. (1995) applied XPS analysis and determined that a passivating film of CuS_2 formed on the surface at low potentials (0.5 V in 1 M $HClO_4$). Further studies by Yin et al. (2000) found chalcopyrite is oxidised, at pH 9.2 with applied potentials of −0.6 to +0.5 V, via a three-stage process. The initial oxidation with potentials <0.02 V formed an iron oxyhydroxide layer, which inhibits further leaching, and CuS_2. The oxidation continues deeper into the material with increased potential from 0.02 to 0.4 V. At potentials greater than 0.4 V the CuS_2 layer decomposes to CuO, S and SO_4^{2-}. Similar iron oxyhydroxide formation has been observed at pH four (Farquhar et al., 2003).

Solution studies by Hiroyoshi et al. (1997, 2001) have observed that chalcopyrite leaching (0.1 M sulfuric acid at 30 °C) was accelerated by the addition of ferrous sulfate. A reaction mechanism involving the reduction of chalcopyrite to Cu_2S followed by subsequent oxidation by ferric ions and release of Cu to solution was proposed. This model was based on solution data alone and no examination of the dissolving surface was undertaken. Thomas et al. (2001) examined the acidic dissolution of pyrrhotite using both solution analysis and time resolved XPS examination of the leach products. They also proposed a dissolution mechanism comprising oxidation and reduction steps. However, it was the oxidation step that was thought to occur initially.

It is apparent, from previous studies, that to understand the mechanism of chalcopyrite dissolution it is essential to determine both solution and surface speciation over the leach duration. To this end, solution and surface studies of a chalcopyrite concentrate leached in perchloric acid ($HClO_4$) were carried out. $HClO_4$ was chosen as the leach agent due to the non-complexing nature of the ClO_4^- anion (Pearson, 1966). Additionally the absence of SO_4^{2-} in the acid enables the observation of S concentration changes in solution throughout the leaches. Although $HClO_4$ is explosive when dry its tendency to be solvated by water means that it provides little oxidising power at the solution concentrations and temperatures used in this study (i.e. below 100 °C and at solution concentrations below 73.6 wt%). It is therefore, a more proficient protonating medium than the more oxidising H_2SO_4 (Pearson, 1966).

2. Methodology

2.1. The chalcopyrite sample

A chalcopyrite concentrate obtained from the KUCC mine in Utah was used. The concentrate was dry sieved to a size fraction of $38 < x < 75$ μm and divided into sample allotments using a separator. Traces of talc, pyrite and sphalerite were detected using powder X-ray diffraction. A total acid digest of the concentrate revealed the sample to be composed of 45.0 mol% S, 21.7 mol% Cu and 22.2 mol% Fe. The remaining 11.1% was made up of impurities such as Si, Mo, Mg, Al, Ca, Pb, Zn, K and As (Table 1). A composition-powder X-ray diffraction reconciliation calculation (using S, Cu, Fe and Si) gives rise to a mass fraction composition of 86% chalcopyrite, 4% pyrite, 1% sphalerite and 9% talc. However, the low concentration of Mg in the sample indicates an overestimation of the percentage of talc present.

2.2. The leach conditions

The chalcopyrite leaches were performed using glass reactor vessels with glass lids containing five ports. The ports on the reactor vessel lids were used to house the stirring impeller, water cooled condenser and Eh and pH probes. To minimise evaporation any unused reactor vessel ports were closed using glass stoppers and the lid was held onto the base of the reactor vessel with a metal clip. The leach experiments were stirred using an overhead stirrer with a four-blade teflon impeller raised to approximately 0.03 m from the base of the leach vessel. The stirring speed was measured using a hand held tachometer and was adjusted to 380 rpm using the gears on the motor. The

Table 1
Elemental composition of a digested chalcopyrite sample

	S	Cu	Fe	Si	Mo	Mg	Al	Ca	Pb	Zn	K	As	Ti	P
Wt%	32.0	29.3	27.6	2.62	0.60	0.59	0.46	0.37	0.34	0.28	0.28	0.27	0.06	0.02
Moles/100 g	1.00	0.46	0.49	0.09	0.01	0.02	0.02	0.01	0.002	0.004	0.01	0.004	0.001	0.001

temperature of the leach solution was maintained at 85 °C using a thermostatically controlled bath filled with silicone oil. The reaction vessels, containing one dm^3 of pH one $HClO_4$ solution were placed in the bath and allowed to equilibrate overnight.

Several leaches were carried out under identical conditions to ensure the reproducibility of the leach experiments. In this case twenty samples, measuring ten ml each (equal portions of solution and solid) were taken throughout the dissolution for inductively coupled plasma atomic emission (ICP-AE) analysis. During the other leach experiments Eh and pH were monitored periodically.

2.3. Surface analysis

The samples removed for surface analysis were placed in plastic tubes, the solids were allowed to settle and the excess liquid was decanted. The samples were then rinsed in clean acid solution to prevent contamination of the surface with species from solution. The samples were frozen in liquid N_2 and stored in a freezer until immediately prior to surface analysis. This procedure has been shown to inhibit significant surface speciation alteration (Smart, 1991).

Each slurry sample was placed onto C tape and transferred to the X-ray photoelectron spectrometer. The lack of sample cooling in the introduction chamber (sample exposure time approximately ten minutes) can result in the loss of some S^0 through sublimation (Briggs and Seah, 1987; Kartio et al., 1992). Powder X-ray diffraction analysis of samples (leached using the identical experimental set-up in pH one H_2SO_4 solution with 12.4 g of added $Fe_2(SO_4)_3$ at 85 °C and a stirring speed of 500 rpm for 144 h) that were stored in the introduction chamber of the X-ray photoelectron spectrometer at a pressure of 10^{-6} Torr for 12 h were found to retain a considerable component of crystalline S^0 (Harmer, 2002). This indicates that the loss of S^0 by exposure to ambient vacuum for ten minutes is likely to be minor.

X-ray photoelectron spectra were recorded using a PHI 5600ci spectrometer with a non-monochromatised Mg Kα irradiation source operating at 300 W. A pass energy of 11.75 eV was used for each spectral scan with an incident X-ray spot size of 1.1 mm^2. All XPS analyses was performed at a detector angle of 45° to the sample so that more than 90% of the electrons emitted were excited from within the top three nm of the sample (Briggs and Seah, 1987). A pressure of 10^{-8} Torr was maintained in the analytical chamber. The sample holder in the analysis chamber was cooled using liquid N_2 for the duration of the experiment.

Carbon cloth (C 1s binding energy of 284.6 eV) was used to calibrate the spectrometer. Each spectral peak position was charge corrected with reference to the adventitious hydrocarbon C 1s binding energy of 284.8 eV (Metson, 1999). Atomic concentrations of Cu, Fe and S were determined from the XPS peak areas, subsequent to Shirley background subtraction, using the elemental sensitivity factors as determined by Wagner et al. (1979). The XPS elemental analyses have been normalised to Cu, Fe and S only (Tables 2 and 3). The major components removed from the elemental accounting by this normalisation process are C in the form of adventitious hydrocarbons and O in the form of H_2O. The S spectra were fitted using the $2p_{1/2}$ and $2p_{3/2}$ doublet in a 1:2 ratio with a separation of 1.18 eV (Buckley and Woods, 1984).

On removal from the freezer the portion of the samples to be examined by scanning electron microscopy (SEM) were thawed, mounted and coated with carbon to ensure conductivity. A Cam Scan 44 FE, with a field emission electron gun was used.

Time of flight secondary ion mass spectrometry (ToF-SIMS) data collection was carried out with a PHI TRIFT II using a pulsed Ga^+ ion beam to sputter and ionise species from the sample surface. Each solid sample was thawed before being dispersed in milli-Q water and mounted on a piece of indium metal that had been taped with carbon tape onto a silica substrate. The samples were then placed into the (ambient) introduction chamber of the ToF-SIMS and evacuated for one hour. ToF-SIMS analysis is considerably more surface sensitive than XPS analysis with a surface sensitivity of one to two monolayers.

Each region of interest (identified manually) within a mass fragment image is divided by the total ion counts across that area (and then multiplied by a scalar of 100) to remove topographical effects. The spectra obtained from the regions of interest were normalised so that the maximum intensity, over all regions of interests, for each species was one. Thereafter the intensities within each region of interest were averaged for each species to give rise to the final species intensities for each region of interest. The number of regions of interest analysed ranged from 8 to 24 depending on the consistency of the samples. Species intensities may be compared between samples but not between species.

Table 2
The variation in binding energy of the C 1s XPS peak during the leaching of chalcopyrite at a pH 1, 85 °C and a stirring speed of 380 rpm

Time (h)	C 1s binding energy (eV) non-charge corrected
0	285.3
2	284.2
24	284.1
144	284.6
313	285.0

Table 3
Total % of Cu, Fe and S present on the surface of chalcopyrite leached in $HClO_4$ at an initial pH of 1 at 85 °C and a stirring speed of 380 rpm (normalised to Cu, Fe and S)

Total % (normalised to Cu, Fe and S)	Unleached	2 h	24 h	144 h	313 h
Fe	59.8	18.1	55.0	9.3	8.8
Cu	14.9	42.6	23.3	13.3	12.8
S	25.3	39.3	21.7	77.3	78.3

3. Results and discussion

3.1. Solution analyses

By 50 h of leaching significantly more Cu had been released to solution than Fe (Fig. 1a) due to the greater rate of leaching of Cu. After 50 h of leaching the release rates of Cu and Fe are approximately equal and both increase with increasing leach time (Fig. 1b). Over the duration of the leach 25% of the total S present in the chalcopyrite was released into solution (Fig. 1b). However, S was observed to sublime and deposit on the underside of the reactor vessel lid by 144 h of leaching.

The Eh of the leach liquor, at a temperature of 85 °C, was measured to be 560 ± 70 mV (SHE). The pH of the leach solution, initially one, slowly increased to 1.6 by the end of the leach. The calculated solution speciation for the Eh, pH and solution concentrations observed over the leach duration is dominated by free Fe^{2+} and Cu^{2+} (MINTEQA2, 1991) with only approximately 1% of either these cations present as $FeSO_{4(aq)}$ or $CuSO_{4(aq)}$.

3.2. XRD analysis

Powder X-ray diffraction was performed on a portion of the solid recovered from the time resolved dissolution experiments. The diffraction patterns obtained were interpreted using Micro Powder Diffraction search/Match © PSI International, Inc. Each diffraction pattern was compared with file patterns from sets one to 44 of the Joint Committee on Diffraction Standards © (JCPDS). Patterns for the samples collected prior to 96 h of leaching showed chalcopyrite, molybdenite and quartz to be present but at 96 h a strong pattern for crystalline S^0 was also apparent. Fig. 2 shows the patterns obtained at two (a) and at 96 h (b).

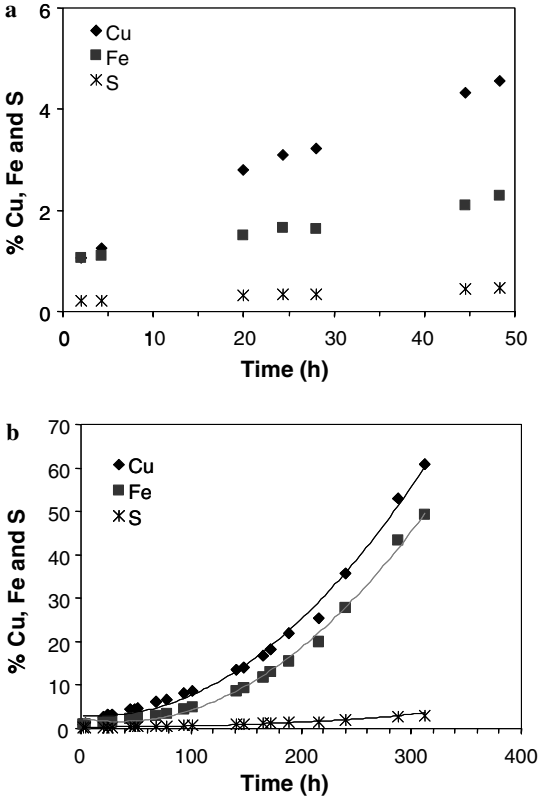

Fig. 1. Cu, Fe and S release from chalcopyrite in $HClO_4$ with an initial pH of 1, a temperature of 85 °C and a stirring speed of 380 rpm for (a) 50 and (b) 313 h (the total duration of the leach).

3.3. SEM analysis

The SEM micrographs collected from particles leached for two and 24 h showed no major signs of reaction merely a few slightly rounded edges (Fig. 3a and b). Particles extracted after 144 h are shown in Fig. 3c and d. On ten-fold increased magnification a bubbly texture is apparent (Fig. 3e), as are small crystallite protrusions indicative of crystalline S^0 (Fig. 3f).

3.4. XPS analysis

3.4.1. Surface charging

The degree and form of surface charging occurring during XPS analysis has been examined by measurement of the binding energy of the C 1s peak as a function of leach duration. With insulating surfaces electrons ejected from the surface are not replaced from 'earth' resulting in the surface having a positive charge. This in turn increases the energy required for electrons to be emitted from the surface and thus the binding energies observed are greater than those for a conducting surface. The C 1s peak of the air oxidised unleached chalcopyrite occurs at 285.3 eV (Table 2) rather than at 284.8 eV. However, chalcopyrite surfaces extracted after two, 24 and 144 h of leaching give rise to a C 1s binding energy less than 284.8 eV implying an excess of surface electrons. The implication is that at these times the dissolving surface of chalcopyrite has a state that can accumulate electrons creating a negatively charged surface. This effect has also been observed with pyrrhotite (Thomas et al., 1998, 2001).

3.4.2. Fe $2p_{3/2}$ spectra

The unleached chalcopyrite surface is dominated by Fe(III)–O–OH at 711 eV (McIntyre and Zetaruk, 1977), with some Fe(III)–S at 707.7 eV (McIntyre and Zetaruk, 1977; Nesbitt and Muir, 1998) (Fig. 4). Similar Fe oxyhydroxide surface layers have been observed previously on air oxidised surfaces of chalcopyrite (Holloway et al., 1982; Buckley and Woods, 1984; Hackl et al., 1995; Klauber et al., 2001; Mikhlin et al., 2004). The decrease in Fe concentration at the surface after 2 h of leaching (Table 3) is due to the removal of Fe(III)–O–OH and the exposure of the Fe-depleted under layer (Mikhlin et al., 2004). After 24 h of leaching the contribution of Fe in the surface has again risen (to 55.0% normalised to Cu, Fe and S) and the majority of this is now as Fe(III)–S (Fig. 4). As the

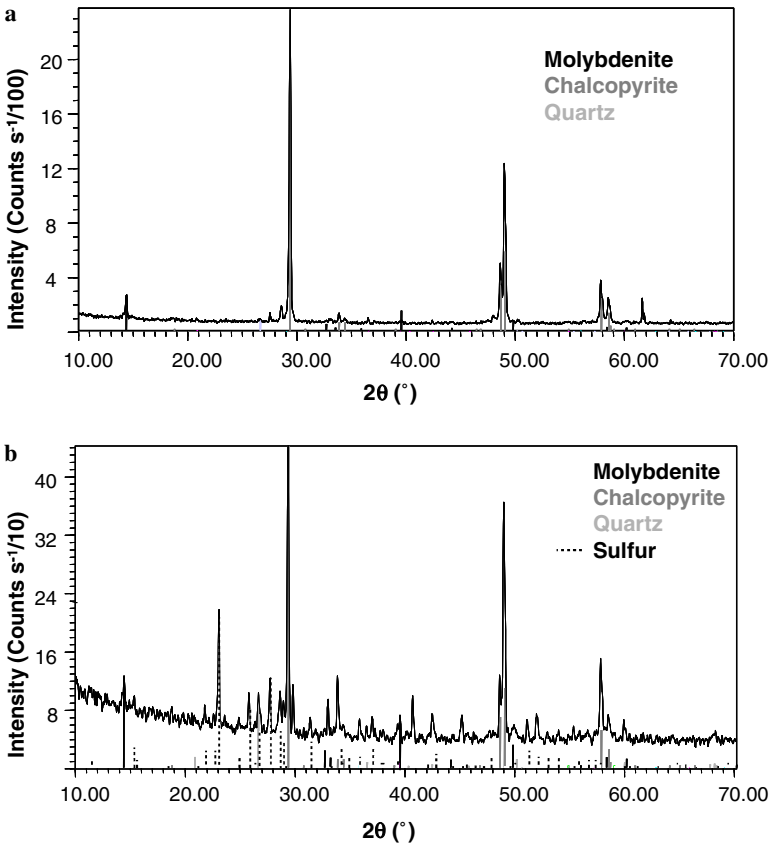

Fig. 2. Powder X-ray diffraction patterns of $CuFeS_2$ leached in $HClO_4$ with an initial pH of one and a temperature of 85 °C, for (a) two h—showing chalcopyrite but no crystalline S^0 and (b) 96 h—showing both chalcopyrite and crystalline S^0.

leach progresses to 144 h the Fe surface component reduces to only 9.3%, still predominantly as Fe(III)–S. The concentration (Table 3) and surface speciation of Fe remains essentially the same between 144 and 313 h (Fig. 4) of leaching.

3.4.3. Cu 2p spectra

The surface of the unleached chalcopyrite consisted of 14.9% Cu (Table 3, normalised to Cu, Fe and S) mostly as Cu(I)-sulfide (932.5 eV) with some $Cu(OH)_2$ (934.2 eV, McIntyre and Cook, 1975; Chawla et al., 1992) and $CuSO_4$ at 934.5 eV (Fig. 5), as confirmed by the SO_4^{2-} peak at about 169 eV (Fig. 6) (Nesbitt and Muir, 1994, 1998). The position of the peak maximum of the Cu $2p_{3/2}$ spectrum after two h of dissolution (Fig. 5) is unchanged from that of the unleached chalcopyrite. The surface concentration of Cu at this time increased to 42.6%, which corresponds to the decrease in Fe. It can therefore be concluded that the Fe(III)–O–OH layer on the unleached surface had decreased to a depth of two nm or less allowing the Cu rich under-layer to be observed using XPS. A similar Cu $2p_{3/2}$ XPS spectrum is also observed after 24 h of leaching but the concentration of Cu on the surface has decreased to 23.3%, with the surface again becoming Fe rich. This decrease in Cu between two and 24 h is consistent with the greater rate of Cu leaching as compared to Fe during this period (Fig. 1a).

After 144 h of leaching the concentration of Cu has decreased to 13.3% (normalised to Cu, S and Fe) and remains at approximately this concentration until the end of the leach. At 144 and 313 h the Cu $2p_{3/2}$ spectrum shows a slight shift to a lower binding energy of 932.3 eV (Fig. 5) due to the formation of Cu(I)–S_n^{2-}. This assignment is based upon comparison with the XPS analysis of synthesised $[Cu(I)_3(S_4)_3]^{3-}$ (courtesy of Prof. Alan Buckley, University of New South Wales) that gave rise to a Cu $2p_{3/2}$ binding energy of 932.3 eV. The $[Cu(I)_3(S_4)_3]^{3-}$ structure consists of both CuS_4 and Cu_3S_3.

3.4.4. S 2p spectra

As both S^0 and metal deficient or S_n^{2-} species have been proposed to be responsible for the passivation of chalcopyrite upon leaching, it was important to obtain reliable binding energy assignments for these species. For this purpose the S 2p spectra of synthetic $[Pt(S_5)_3]^{2-}$ (provided by Prof. Alan Buckley, University of New South Wales) as well as $[Cu(I)_3(S_4)_3]^{3-}$ were analysed using XPS. The $[Pt(S_5)_3]^{2-}$ structure consists of both PtS_5 and PtS moieties. XPS analysis found the S $2p_{3/2}$ binding energies to be at 161.8 eV for S^{2-} and 163.0 eV for S_n^{2-} for the $[Cu(I)_3(S_4)_3]^{3-}$ sample, and 162.0 and 163.2 eV, respectively, for the $[Pt(S_5)_3]^{2-}$ sample (Harmer, 2002). XPS binding energies of these and related materials are also reported by Termes et al. (1987) and Chawla et al. (1992). The S $2p_{3/2}$ binding energy

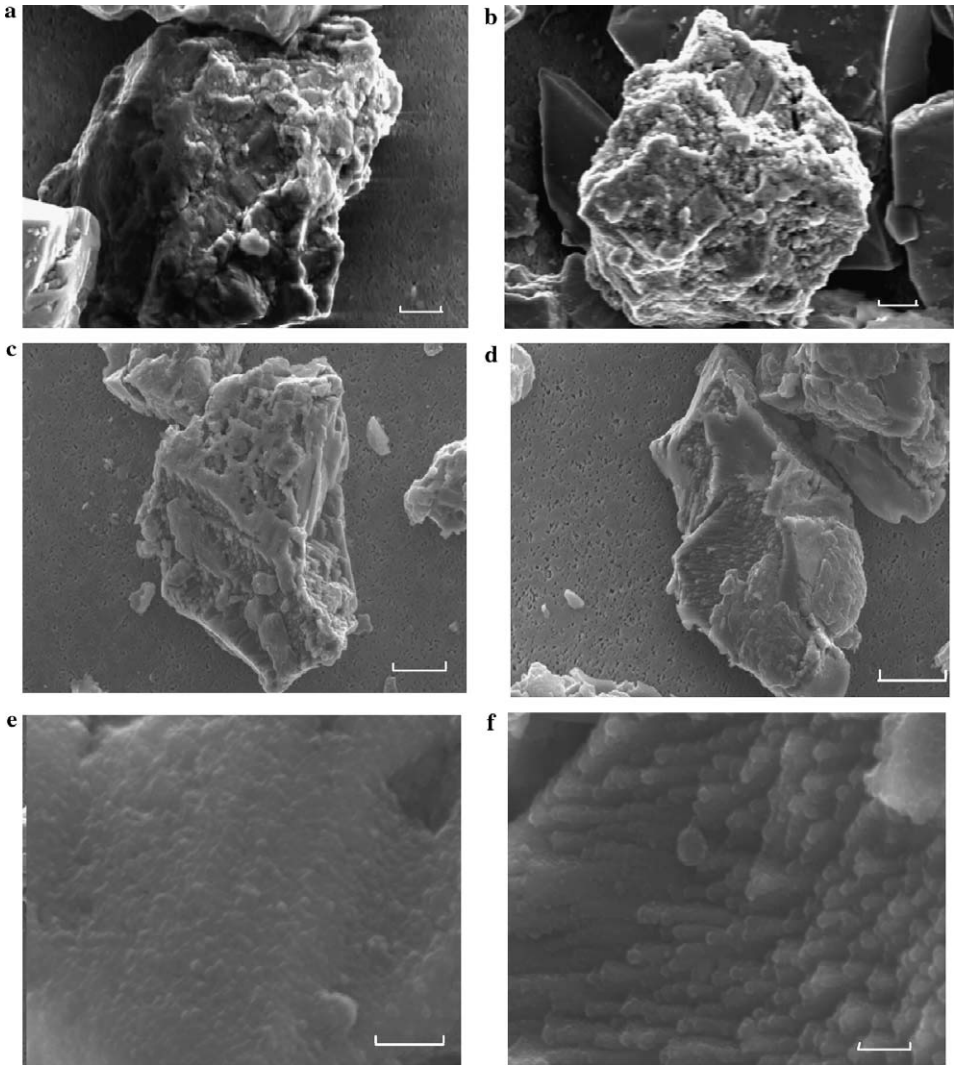

Fig. 3. SEM images of chalcopyrite particles after leaching in pH one $HClO_4$ at 85 °C; (a) after two, (b) after 24 and (c) and (d) after 144 h, one scale unit = ten μm; (e) and (f) after 144 h, one scale unit = ten μm.

for S_n^{2-} was allowed to range between 163.0 and 163.9 eV during fitting of the XPS data. A doublet representing S^0 has been fitted to the spectra arising from the samples leached for 144 and 313 h (Fig. 6) at S $2p_{3/2}$ binding energy of 164.1 eV (Nesbitt and Muir, 1998). S_n^{2-}, S^0 these times correspond to the visual observation of S^0 crystals on the lid of the reactor vessel.

During the first two h of leaching, the total concentration of S species increased from 25.3% to 39.3% (normalised to Cu, Fe and S, Table 3), corresponding to the decrease in surface Fe(III)–O–OH during this period. The SO_4^{2-} present on the unleached sample (Table 4, Fig. 6) is removed from the surface. The concentrations of both S_2^{2-} and S_n^{2-} increase (Table 4, Fig. 6).

The total surface concentration of S was 21.7% (relative to Cu, Fe and S) after 24 h of leaching which increased dramatically to 77.3% on 144 h of leaching. A significant increase in leach rate is observed over this period (Fig. 1 (b)). The S 2p XPS spectrum of the sample leached for 144 h indicates a combination of S^{2-}, S_2^{2-}, S_n^{2-} and S^0. The concentration of S^{2-} increases from 5.9% at 24 h to 17.7% at 144 h. The S concentration and speciation on the surfaces after 144 and 313 h of leaching are very similar. As the concentration of S increases on the surface for the duration of the leach and the leach rate increases, it is apparent that the formation of neither S^0 nor S_n^{2-} is passivating.

3.4.5. O 1s spectra

The unleached sample surface exhibits hydroxyl (OH^-) species at the O 1s binding energy of 530.5 eV and attached H_2O at about 533 eV, Fig. 7 (Nesbitt and Muir, 1994; Legrand et al., 1997). After the first two h of leaching the OH^- contribution decreased significantly. This supports the idea that the Fe(III)–O–OH are one of the first species to be removed and its removal determines the initial Cu leach rate (Table 5). After 24 h, the atomic O concentration rose to 88 at.% before decreasing to 51.55 at.% after 144 h

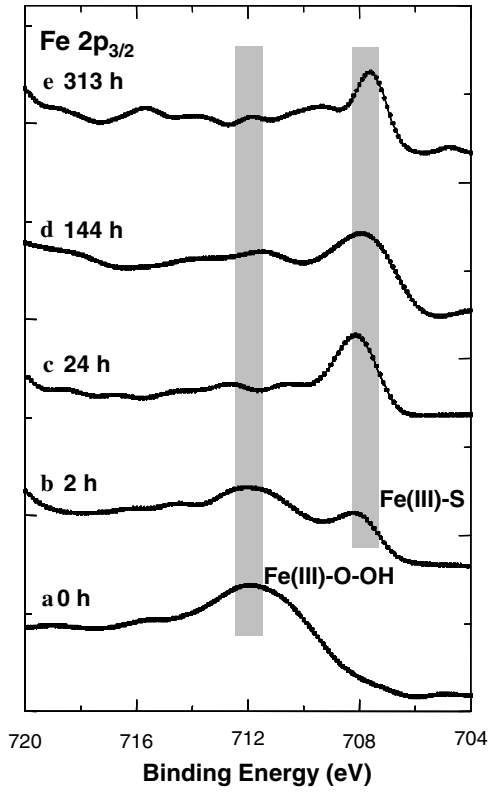

Fig. 4. Normalised XPS Fe 2p spectra of the chalcopyrite (a) unleached, (b) leached for two, (c) 24, (d) 144 and (e) 313 h.

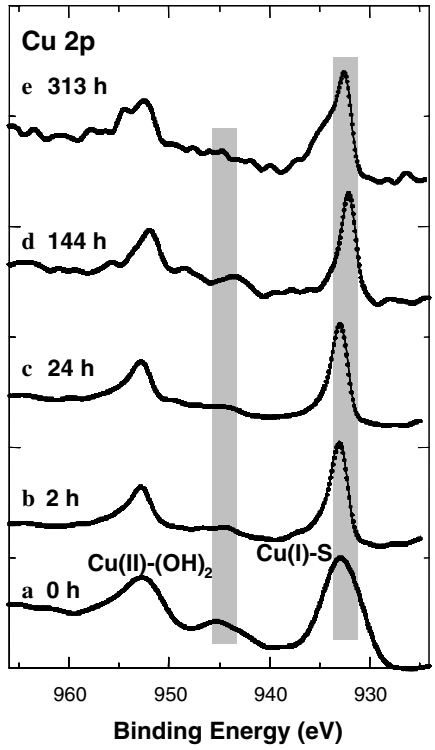

Fig. 5. Normalised XPS Cu 2p spectra of the chalcopyrite (a) unleached, (b) leached for two, (c) 24, (d) 144 and (e) 313 h.

and 53.2 at.% after 313 h. These spectra showed the majority of the species present on the surface were attached and absorbed H_2O.

3.5. ToF-SIMS

Fig. 8a indicates that Fe dominates the ToF-SIMS elemental overlay image of the surface of the unleached chalcopyrite particles. The Fe is highly correlated to the distribution of OH (not shown). After two and 24 h of leaching the components of Cu and S have increased (Fig. 8b and c) as compared to the unleached sample. The increase in S between two and 24 h is statistically significant (Fig. 9a). XPS analysis indicates a decrease in the surface composition of S and Cu during between two and 24 h of leaching. These contrasting results indicate that at 24 h of leaching the Cu-rich sulfide layer has not been completely removed but is sufficiently thin for the XPS signal to be dominated by the underlying speciation. There exists a statistically significant decrease in the concentration of Cu, and increase in Fe, between 24 and 144 h (Fig. 9b) corresponding to the complete removal of the Cu-rich sulfide layer. After 144 and 313 h (Fig. 8d and e) the particles are beginning to break down and holes are apparent.

4. Summary of surface layer changes

The changes to the surface of the chalcopyrite during leaching are illustrated diagrammatically in Fig. 9. The initial surface of the chalcopyrite, prior to leaching (Fig. 8a), is Fe rich and comprised of OH^- and SO_4^{2-}.

Within two h of leaching (Fig. 10b) the Fe(III)–O–OH surface layer had begun to be removed (thinning and possibly forming islands) revealing a Cu(I) rich sulfide layer. The overall concentration of S has increased but SO_4^{2-} has been removed and the concentration of S^{2-} decreased. An increase in S_2^{2-} and S^{2-} is observed.

By 24 h of leaching (Fig. 10c) all of the Fe(III) oxyhydroxide has been removed from the surface. In the period from two to 24 h the concentration of Fe has increased and is primarily in the form of Fe(III)-sulfide, from the chalcopyrite layer underlying the remaining Cu(I) rich sulfide. The rate of Cu leaching in this time period is greater than the rate of Fe leaching, supporting the presence of a Cu rich outermost layer.

Upon further leaching to 144 h (Fig. 10d) the surface concentrations of Cu and Fe become approximately the same. The surface layer is composed of Fe(III) and Cu(I) S^{2-}, S_2^{2-} and S_n^{2-} as well as crystalline S^0. In the period from 24 to 144 h the surface S content increases dramatically. The concentration of S^{2-} significantly increases, as does the concentration of S_n^{2-}. The increasing S_n^{2-} is associated with increasing rates of Cu and Fe release to solution, but little or no release of S to solution. The increased concentration of S^{2-} in this period may be explained by the occurrence of a reduction step to form lower oxidation state S species and shorter chain S_n^{2-}. Such a step has been proposed by Thomas et al. (2001) for the dissolution of pyrrhotite in acidic conditions. An alternative explanation for the increase in surface S^{2-} at 144 h of leaching may be that oxidized surface species have been

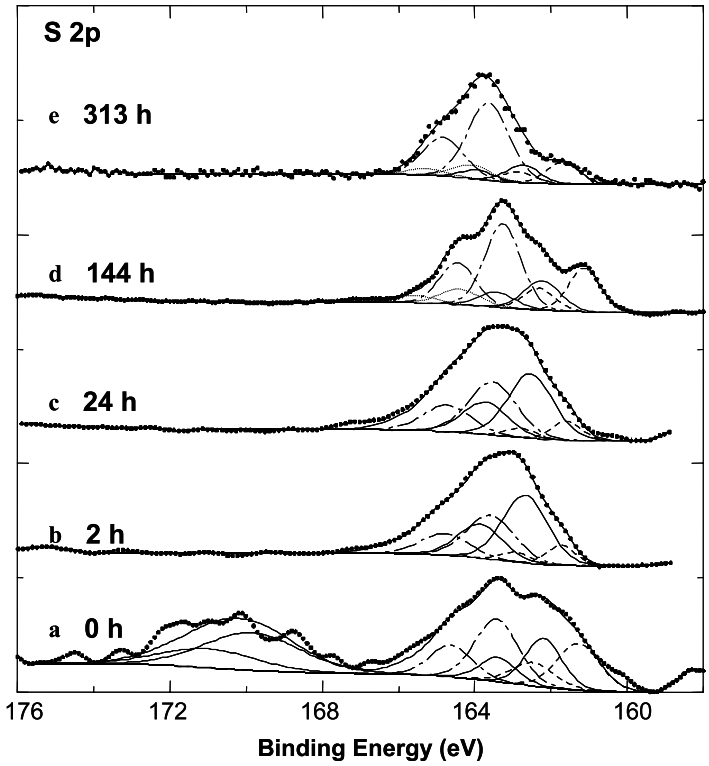

Fig. 6. Normalised XPS S 2p spectra for chalcopyrite (a) unleached, (b) leached for two, (c) 24, (d) 144 and (e) 313 h. Fits have been provided for S^{2-} (dashed line), S_2^{2-} (solid line), S_n^{2-} (dash dotted line), S^0 (dotted line) and SO_4^{2-} (solid line).

Table 4
Binding energy and atomic percent of S species present on the surface of chalcopyrite leached in $HClO_4$ at an initial pH of one at 85 °C and a stirring speed of 380 rpm (normalised to Cu, Fe and S)

Species	S $2p_{3/2}$ binding energy (eV)[a]	Unleached	2 h	24 h	144 h	313 h
S^{2-}	161.4	12.6	5.8	5.9	17.7	11.0
S_2^{2-}	162.4	5.2	15.3	8.3	13.7	9.2
S_n^{2-}	163.0–163.9	2.3	18.2	7.5	38.2	49.8
S^0	164.1	0.0	0.0	0.0	7.7	8.3
SO_4^{2-}	168.5	5.2	0.0	0.0	0.0	0.0
Total S %		25.3	39.3	21.7	77.3	78.3

[a] Nesbitt and Muir (1998).

removed to reveal bulk chalcopyrite. However, this hypothesis is not favoured due to the negative shift in binding energy of the Cu $2p_{3/2}$ spectrum, collected after 144 h, to that observed for a synthetic Cu–S_n^{2-}, the observation of the formation of crystallites on the leached surfaces coinciding with the emergence of S^0 species and the reduction in binding energy of the XPS C1s spectral component for adventitious C.

Between 144 and 313 h of leaching the rate of leaching of both Cu and Fe continues to increase, with little increase in solution S concentration. There is little change in the concentrations or speciation of Cu, Fe and S on the surface.

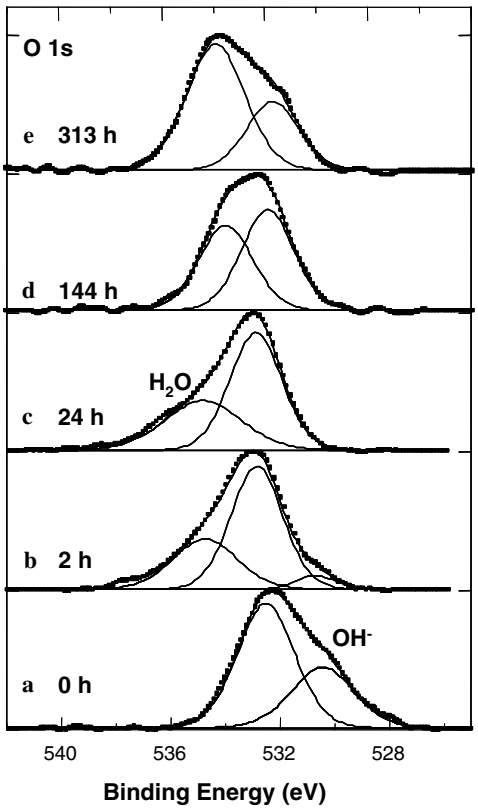

Fig. 7. Normalised XPS O 1s spectra for chalcopyrite (a) unleached, (b) leached for two, (c) 24, (d) 144 and (e) 313 h.

Table 5
Binding energies and atomic percent of O species present on the surface of $CuFeS_2$ leached in $HClO_4$ at an initial pH of one at 85 °C and a stirring speed of 380 rpm (normalised to Cu, Fe, S and O)

Species	Binding energies O 1s (eV)[a]	Unleached	2 h	24 h	144 h	313 h
OH^-	530.5–531.5	27.2	4.1	0.0	0.0	0.0
Attached H_2O	532–533.5	50.8	47.6	54.1	27.6	17.5
Adsorbed H_2O	534–538	0.0	24.4	33.9	23.9	35.7
Total O % (normalised to Cu, Fe, S and O)		78.0	76.1	88.0	51.5	53.2

[a] (Nesbitt and Muir, 1994; Legrand et al., 1997; Yin et al., 2000).

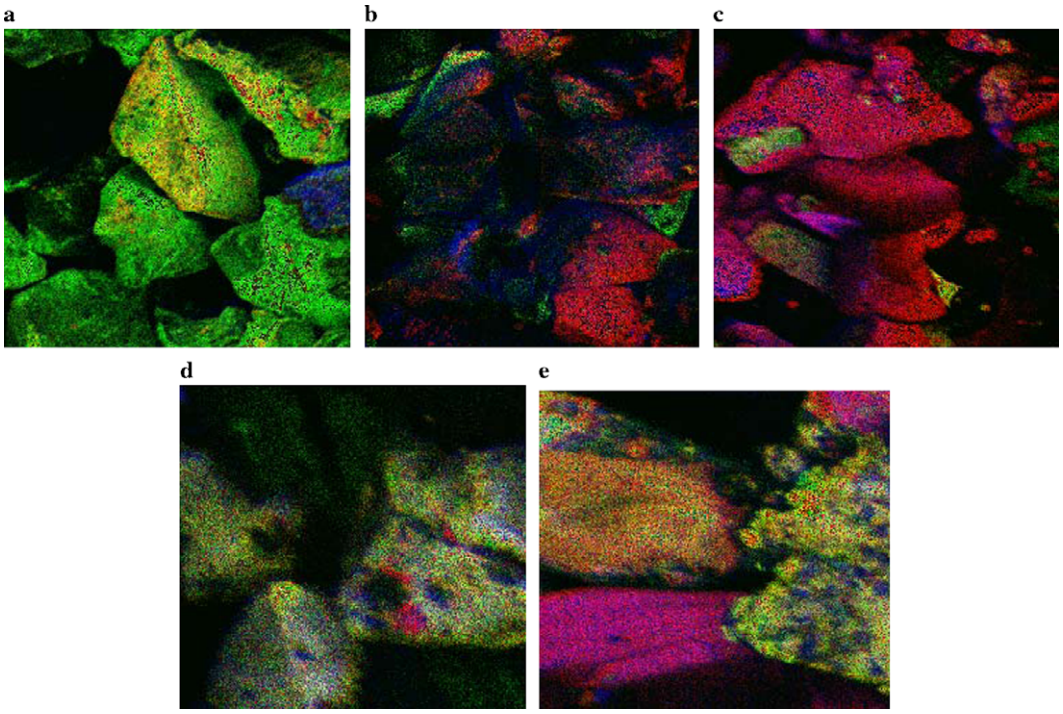

Fig. 8. ToF-SIMS elemental overlays of Cu (red), Fe (green), S (blue) of (a) unleached chalcopyrite, (b) after leaching for two, (b) 24, (c) 144 and (d) 313 h. The width of each image is 100 μm.

5. Proposed reaction pathway

In order to account for the experimental observations described a reaction pathway allowing 100% release of Cu from chalcopyrite is proposed. The reaction pathway includes both oxidation and reduction steps but differs from that of Hiroyoshi et al. (2001) who proposed a reduction step prior to oxidation. The development of the model by Hiroyoshi et al. (2001) did not include surface analytical studies and thus did not take into account changes in surface speciation. Thus, the initial formation of S_n^{2-} (evidence of oxidation) and the later re-emergence of S^{2-} species were not taken into account, nor was the formation of crystalline S^0.

The initial stages of the proposed reaction pathway involve the dissolution of SO_4^{2-} and Fe(III)–O–OH species from the surface. The reduction of Fe^{3+} to $Fe^{2+}_{(aq)}$ oxidises the underlying Cu rich layer resulting in the formation of S_n^{2-} and the release of Cu^+ and Fe^{2+}. Since there was no evidence of Cu^{2+} on the surface of the chalcopyrite samples extracted during leaching, it is proposed that oxidation of Cu^+ to Cu^{2+} occurs in solution immediately upon release. The overall equation describing this step is given in Eq. (1).

$$(12n-12)Fe^{3+}_{(aq)} + 3nCuFeS_{2(solid)} \rightarrow [4(CuFe)^{4+}\cdot 6(S_n^{2-})]_{(solid)} + (3n-4)Cu^{2+}_{(aq)} + (15n-16)Fe^{2+}_{(aq)} \quad \text{where } n \geqslant 2 \tag{1}$$

It can be seen from Eq. (1) that the extent of S_n^{2-} formation is a function of the % Cu and Fe released. Many previous studies have equated the formation of a S rich surface layer with the slowing of the rate of Cu release. This was not observed in this study. It is proposed that, if conditions allow, a reduction step results in the conversion of S_n^{2-} to S^{2-} (Eq. (2)) or other short chain S_n^{2-}. This reaction is driven by the oxidation of Fe^{2+} to Fe^{3+} and involves adsorption of H^+ from solution in order to balance the resulting surface charge. This step then accounts for the increase in pH observed over the

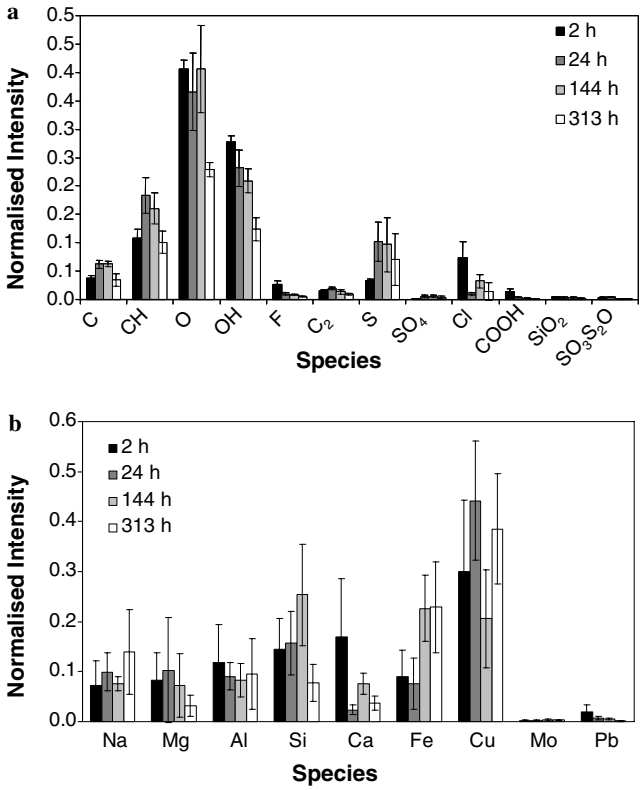

Fig. 9. Comparison of ToF-SIMS ion yield normalised intensities for (a) −ve and (b) +ve species as measured on chalcopyrite samples leached at 85 °C at 380 rpm and an initial pH of one in $HClO_4$.

duration of the leach. Two alternatives for the resulting leached chalcopyrite structure are given in Eq. (2) to demonstrate the possible formation of a mixture of S^{2-} product and H_2S (some H_2S release was observed during chalcopyrite leaching). The reduction of the S_n^{2-} layer does not result in the release Cu and Fe from the solid but does enable an oxidation reaction to form crystalline S^0 to proceed (Eq. (3)). This second oxidation step involves a massive structural rearrangement of the surface to form crystallites of S^0. It is proposed that this rearrangement is not possible directly from amorphous long-chain S_n^{2-} but must proceed through the shorter chain S building blocks.

$$\begin{aligned}&[4(CuFe)^{4+}\cdot 6(S_n^{2-})]_{(solid)} + (12n-12)Fe^{2+}_{(aq)}\\&\quad + (12n-12)H^{+}_{(aq)} \rightarrow [4(CuFe)^{4+}\cdot(6n-6)H_2S\cdot 6(S^{2-})]_{(solid)}\\&\quad + (12n-12)Fe^{3+}_{(aq)}\\&and/or\\&\quad \rightarrow [4(CuFe)^{4+}\cdot(12n-12)H^{+}\cdot 6n(S^{2-})]_{(solid)}\\&\quad + (12n-12)Fe^{3+}_{(aq)} \quad \text{where } n \geqslant 2\end{aligned} \tag{2}$$

$$\begin{aligned}&[4(CuFe)^{4+}\cdot(12n-12)H^{+}\cdot 6n(S^{2-})]_{(solid)}\\&\quad + (12n)Fe^{3+}_{(aq)} \rightarrow 6nS^{0}_{(solid)}\ 4Cu^{2+}_{(aq)}\\&\quad + (12n+4)Fe^{2+}_{(aq)} + (12n-12)H^{+}_{(aq)} \quad \text{where } n \geqslant 2\end{aligned} \tag{3}$$

In the proposed reaction pathway the reduction step involving Fe^{2+} in turn regenerates Fe^{3+} and thus creates a cycle of oxidation and reduction. The proposed reaction pathway is consistent with the observations of Fe^{2+} promoted chalcopyrite leaching (Hiroyoshi et al., 1997, 2000).

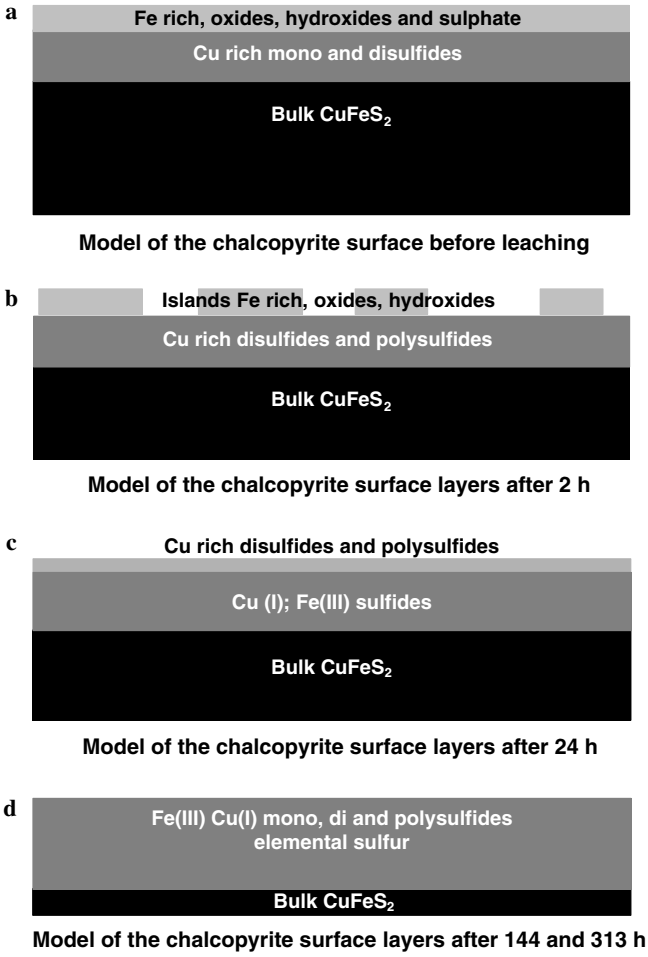

Fig. 10. Model of the surface changes observed on chalcopyrite during leaching at 85 °C at an initial pH of one in $HClO_4$ with 380 rpm stirring.

Acknowledgments

The authors of this paper acknowledge Rio Tinto for their financial support. Dr. Peter Anderson and Dr. Ray Shaw are thanked for their helpful discussions and Mr. Angus Netting, Mr. Marek Jasieniak and Mr. Len Green are thanked for their assistance with the surface analytical techniques featured in this paper. Assoc. Prof. Alan Buckley (University of New South Wales) is thanked for supplying synthetic polysulfides. We also thank the reviewers and editors of the manuscript including Dr. Michael Borda and Prof. David Vaughan.

Associate editor: David J. Vaughan

References

Barriga, M.F., Palencia, P.I., Carranza, M.F., 1987. The passivation of chalcopyrite subjected to ferric sulfate leaching and its reactivation with metal sulfides. *Hydrometallury* **19**, 159–167.

Biegelsen, D.K., Bringans, R.D., Northrup, J.E., Swartz, L.E., 1990. Reconstructions of GaAs ($\overline{111}$) surfaces observed by scanning tunnelling microscopy. *Phys. Rev. Lett.* **65**, 452–455.

Briggs, D., Seah, M.P., 1987. *Practical surface analysis by Auger and X-ray photoelectron spectroscopy*. John Wiley & Sons.

Buckley, A.N., Woods, R., 1984. An X-ray photoelectron spectroscopic study of the oxidation of chalcopyrite. *Aust. J. Chem.* **37**, 2403–2413.

Chawla, S.K., Sankarraman, N., Payer, J.H., 1992. Diagnostic spectra for XPS analysis of copper-oxygen-sulfur-hydrogen system compounds. *J. Electron Spectrosc. Related phen.* **61**, 1–18.

Dutrizac, J.E., 1989. Elemental sulfur formation during the ferric sulfate leaching of chalcopyrite. *Can. Metall. Quart.* **28**, 337–344.

Farquhar, M.L., Wincott, P.L., Wogelius, R.A., Vaughan, D.J., 2003. Electrochemical oxidation of the chalcopyrite surface: an XPS and AFM study in solution at pH 4. *Appl. Surf. Sci.* **218**, 34–43.

Hackl, R.P., Dreisinger, D.B., Peters, E., King, J.A., 1995. Passivation of chalcopyrite during oxidative leaching in sulfate media. *Hydrometallurgy* **39**, 25–48.

Harmer, S.L., 2002. *Surface layer control for improved copper recovery for chalcopyrite leaching*. Thesis, Ian Wark Research Institute, University of South Australia.

Harmer, S.L., Pratt, A.R., Nesbitt, H.W., Fleet, M.E., 2004. Sulfur species at chalcopyrite ($CuFeS_2$) fracture surfaces. *Am. Mineral.* **89**, 1026–1032.

Hiroyoshi, N., Hirota, M., Hirajima, T., Tsunekawa, M., 1997. A case of ferrous sulfate addition enhancing chalcopyrite leaching. *Hydrometallurgy* **47**, 37–45.

Hiroyoshi, N., Miki, H., Hirajima, T., Tsunekawa, M., 2001. A model for ferrous-promoted chalcopyrite leaching. *Hydrometallurgy* **57**, 31–38.

Holloway, P.H., Remond, G., Schwartz, W.E., 1982. *Interfacial phenomena in mineral processing*. Engineering Foundation, New York, pp. 3–17.

Kartio, I., Laajalehto, K., Suoninen, E., Karthe, S., Szargan, R., 1992. Technique for XPS measurement of volatile absorbed layers: application to studies of sulfide flotation. *Surf. Interface Anal.* **18**, 807–810.

Klauber, C., Parker, A., Bronswijk, W.V., Watling, H., 2001. Sulphur speciation of leached chalcopyrite surfaces as determined by X-ray photoelectron spectroscopy. *Int. J. Miner. Process.* **62**, 65–94.

Legrand, D.L., Bancroft, G.M., Nesbitt, H.W., 1997. Surface characterization of pentlandite, $(Fe,Ni)_9S_8$ by X-ray photoelectron spectroscopy. *Int. J. Miner. Process.* **51**, 217–228.

Linge, H.G., 1976. A study of chalcopyrite dissolution in acidic ferric nitrate by potentiometric titration. *Hydrometallurgy* **2**, 51–64.

Linge, H.G., 1977. Reactivity comparison of Australian chalcopyrite concentrates in acidified ferric solution. *Hydrometallurgy* **2**, 219–233.

Maurice, D., Hawk, J.A., 1998. Ferric chloride leaching of mechanically activated chalcopyrite. *Hydrometallurgy* **49**, 103–123.

McIntyre, N.S., Cook, M.G., 1975. X-ray photoelectron studies on some oxides and hydroxides of cobalt, nickel and copper. *Anal. Chem.* **47**, 2208–2213.

McIntyre, N.S., Zetaruk, D.G., 1977. X-ray photoelectron spectroscopic studies of iron oxides. *Anal. Chem.* **49**, 1521–1529.

Metson, J.B., 1999. Charge compensation and binding energy referencing in XPS analysis. *Surf. Interface Anal.* **27**, 1069–1072.

Mikhlin, Y.L., Tomashevich, Y.V., Asanov, I.P., Okotrub, A.V., Varnek, V.A., Vyalikh, D.V., 2004. Spectroscopic and electrochemical characterization of the surface layers of chalcopyrite ($CuFeS_2$) reacted in acidic solutions. *Appl. Surf. Sci.* **225**, 395–409.

MINTEQA2, 1991. *Metal speciation equilibrium model for surface and ground water*. Version 3.11, Center for Exposure Assessment Modeling (CEAM), U.S. Environmental Protection Agency, Office of Research and Development, Environmental Research Laboratory, College Station Road, Athens Georgia 30613-0801.

Munoz, P.B., Miller, J.D., Simkovich, G., 1984. Enhanced ferric sulphate leaching of copper from $CuFeS_2$ and C particulate aggregates. In: Jaughton, L.F. (Ed.), *Mintek 50 International Conference on Mineral Science and Technology*. The Council for Mineral Technology, Randburg, South Africa, pp. 575–588.

Nesbitt, H.W., Muir, I.J., 1994. X-ray photoelectron spectroscopic study of a pristine pyrite surface reacted with water vapour and air. *Geochim. Cosmochim. Acta* **58**, 4667–4679.

Nesbitt, H.W., Muir, I.J., 1998. Oxidation states and speciation of secondary products on pyrite and arsenopyrite reacted with mine waste waters and air. *Mineral. Petrol.* **62**, 123–144.

Nesbitt, H.W., Reinke, M., 1999. Properties of As and S at NiAs, NiS and $Fe_{1-x}S$ surfaces, and reactivity of niccolite in air and water. *Am. Mineral.* **84**, 639–649.

O'Malley, M.L., Liddell, K.C., 1986. The rate equation for the initial stage of the leaching of chalcopyrite by aqueous $FeCl_3$ HCL and NaCl. *The Metallurgical Society Inc. Symposium* 67–97.

Parker, A., Klauber, C., Kougianos, A., Watling, H.R., van Bronswijk, W., 2003. An X-ray photoelectron spectroscopy study of the mechanism of oxidative dissolution of chalcopyrite. *Hydrometallurgy* **71**, 265–276.

Pearson, G.S., 1966. Perchloric acid. *Advances in Inorganic Chemistry and Radiochemistry* **8**, 177–224.

Prasad, S., Pandey, B.D., 1998. Alternative processes for treatment of chalcopyrite-a review. *Miner. Eng.* **11** (8), 763–781.

Smart, R.St.C., 1991. Surface layers in base metal sulfide flotation. *Miner. Eng.* **4**, 891–909.

Termes, S.C., Buckley, A.N., Gillard, R.D., 1987. 2p electron binding energies for sulfur atoms in metal polysulfides. *Inorg. Chem. Acta* **126**, 79–82.

Thomas, J.E., Jones, C.F., Skinner, W.M., Smart, R.St.C., 1998. The role of sulfur species in the inhibition of pyrrhotite dissolution in acid conditions. *Geochem. Cosmochem. Acta* **62**, 1555–1565.

Thomas, J.E., Skinner, W.M., Smart, R.St.C., 2001. A mechanism to explain sudden changes in rates and products for pyrrhotite dissolution in acid conditions. *Geochim. Cosmochim. Acta* **65**, 1–12.

Wagner, C.D., Riggs, W.M., Davis, L.E., Moulder, J.F., Muillnbery, G.E. (Eds.), 1979. *Handbook of X-ray Photoelectron Spectroscopy*. Perkin Elmer Corporation, Eden Prairie, Minn. USA.

Yin, Q., Kelsall, G.H., Vaughan, D.J., England, K.E.R., 1995. Atmospheric and electrochemical oxidation of the surface of chalcopyrite ($CuFeS_2$). *Geochim. Cosmochim. Acta* **59**, 1091–1100.

Yin, Q., Vaughan, D.J., England, K.E.R., Kelsall, G.H., Brandon, N.P., 2000. Surface oxidation of chalcopyrite ($CuFeS_2$) in alkaline solutions. *J. Electrochem. Soc.* **147**, 2945–2951.